Diffusion-Weighted MR in Experimental Sustained Seizures Elicited with Kainic Acid

Y. Nakasu, S. Nakasu, S. Morikawa, S. Uemura, T. Inubushi, and J. Handa

PURPOSE: To investigate the early changes in diffusion-weighted MR images in the sustained limbic seizures. **METHOD:** Intraperitoneal injection of kainic acid was used to induce sustained limbic seizures in seven rats. The animals were investigated with serial 2.0-T MR imaging beginning immediately after kainic acid–induced seizures, and at 24 hours, 3 days, and 7 days after the kainic acid injection. Diffusion-weighted spin-echo and T2-weighted images and apparent diffusion coefficients were sequentially assessed and compared with histologic changes. The results were compared with eight control animals given buffered saline intraperitoneally. **RESULTS:** Diffusion-weighted MR images revealed an increase in signal intensity bilaterally in the amygdala and the piriform cortices immediately after the sustained seizures, whereas T2-weighted images did not show changes in signal intensity at this time. Both diffusion-weighted and T2-weighted images showed marked increase in signal intensities in these same areas 24 hours after kainic acid injection. The apparent diffusion coefficient values were significantly lower in the area of the amygdala and the piriform cortex immediately after and lower again 24 hours after the sustained seizures. The area of hyperintensity in diffusion-weighted images was concordant with the histologic distribution of neuronal pyknosis and neuropile vacuolation. **CONCLUSION:** Diffusion-weighted MR revealed focal abnormalities in the limbic system after 1 hour of sustained seizures induced with kainic acid, before changes on T2-weighted imaging. Diffusion-weighted MR is a potential method for studying the mechanisms of brain damage caused by sustained seizures.

Index terms: Brain, effects of drugs on; Magnetic resonance, diffusion-weighted; Seizures; Animal studies

AJNR Am J Neuroradiol 16:1185–1192, June 1995

Magnetic resonance (MR) imaging is the examination of choice in the differential diagnosis of focal organic lesions in the brains of patients with epilepsy. Furthermore, several authors reported transient focal abnormalities demonstrated with MR images during and after clinical status epilepticus: focal brain regions with high signal intensity on T2-weighted (T2W) spin-echo images (1, 2), or abnormal gadopentetate dimeglumine enhancement (3, 4). The abnormal MR findings were ascribed to transient focal vasogenic edema and hypervascularisation induced by sustained epileptic seizures. However, few in vivo MR imaging studies have been done in experimental seizure models of status epilepticus (5, 6). Diffusion-weighted (DW) spin-echo MR imaging has been applied for imaging brain abnormalities made by microinjection of excitatory amino acids and by systemic treatment with γ-aminobutyric acid receptor blocker under general anesthesia (7–9). Early detection of abnormal areas in ischemic brain with DW MR imaging has presented a superior sensitivity to conventional T2W MR imaging (10–13). The morphologic pattern of cell damage induced by seizures is in part similar to neuronal alterations after cerebral ischemia, in which excitatory amino acids play an important role in elucidating the excitotoxic process (14). It raises questions about the relation of an acute specific fea-

Received August 19, 1994; accepted after revision January 26, 1995.

Supported in part by Grants-in-Aid No. 05671155 (Y.N.) and No. 06557145 (T.I.) from the Ministry of Education, Science and Culture of Japan, and by a grant (Y.N.) from Japan Epilepsy Research Foundation.

From the Department of Neurosurgery (Y.N., S.N., J.H.) and the Institute of Molecular Neurobiology (S.M., S.U., T.I.), Shiga University of Medical Science, Ohtsu, Japan.

Address reprint requests to Y. Nakasu, MD, Department of Neurosurgery, Shiga University of Medical Science, Seta, Ohtsu, Shiga 520-21, Japan.

AJNR 16:1185–1192, Jun 1995 0195-6108/95/1606–1185

ture of proton diffusion to the brain damage induced by prolonged seizures. Our working hypothesis is that DW MR may be useful in demonstrating in vivo acute focal changes caused by systemic sustained seizures when conventional MR shows no changes in the brain.

We examined the limbic structures of well-oxygenated rats periodically after prolonged seizures elicited by systemic injection of kainic acid (KA). This chemical is a pyrolidine derivative that acts as a direct agonist at glutamate receptors and has a predilection for the limbic system (15). The experimental seizures induced with KA are particularly useful as a model for human temporal epilepsy (16). A recent study has provided a change in signal intensity of the amygdala and piriform cortex in a rat limbic seizure model on T2W images (6).

Methods

Fifteen male Sprague-Dawley rats weighing 280 to 350 g were housed in groups of 2 to 3 per cage in a room with a controlled light-dark cycle (12 hours light and 12 hours dark) and temperature at 23°C. Eight of 15 rats were assigned to the control group with saline injection, and 7 were treated with KA. In all seven animals that received KA, limbic status epilepticus developed, and all were included in MR studies. The experimental procedures strictly followed the guidelines of the animal experiment committee of Shiga University of Medical Science.

Unanesthetized rats were injected intraperitoneally with 12 mg/kg KA (n = 7). All rats treated with KA exhibited progressive limbic seizures within 1 hour after KA injection. The onset of convulsive seizures occurred between 90 and 120 minutes after injection. They were prepared for MR studies about 1 hour after the initiation of convulsive status epilepticus. Eight control animals were treated with corresponding amounts of buffered saline and were examined with MR imaging 2 hours after the injection. Anesthesia for the MR studies was induced with 4% halothane, and maintained with 1.8% halothane in 0.5 to 0.8 L/min oxygen, because preliminary experiments indicated that this level of anesthesia maintained stable physiologic conditions with spontaneous regular breathing and precluded the motion of animals in the magnet while still allowing electrical seizures to occur. The animals were allowed to breathe spontaneously with a face mask in a prone position throughout the imaging. Arterial blood samples were collected from three of the rats with seizures and three in the control group for analysis of blood gases at the baseline, immediately after the induction of anesthesia after sustained seizures, and at the end of the MR study.

The seven KA-treated rats were examined with MR immediately after the 1-hour sustained seizures, and 24 hours, 3 days, and 7 days after the injection of KA. MR imaging was performed in a 2.0-T Omega system (General Electric NMR Instruments, Fremont, Calif) operating at 85.5 MHz for protons. Images were acquired with a homemade 5-cm-diameter radio frequency coil in the magnet fitted with shielded gradients (14 G/cm). A coronal plane was chosen from a sagittal scout view to encompass the center of the amygdala and the dorsal hippocampus in one image. The coronal scan thickness was 2 mm. We also selected a 1-mm-thick horizontal (axial) section through the dorsal hippocampus. This anatomic structure comprises a characteristic thin horizontal plate with multidirectional arrangement of nerve cells and fibers in rats. DW spin-echo images were acquired using a standard T2W sequence incorporating pulsed gradients, based on the method described by Moseley et al (17). The diffusion-sensitizing gradients were applied in the vertical direction for coronal sections and in the horizontal direction for axial sections.

The animals had coronal and axial spin-echo 1800/78/4 (repetition time/echo time/excitations) images with 128 phase-encoding steps. The field of view was 4.5 cm. All data were zero filled to 256 × 256 before processing. Total study time was 90 to 120 min inclusive for a scout image and T2W and DW images. A single b value of 1144 s/mm^2 was used throughout in the DW sequences, yielding heavily diffusion-weighted images. The DW and T2W images were reviewed, and region-of-interest delineation was performed by an operator (S.N.) who was unaware of the kind of treatment. The average size for each of the regions of interest follows.

	Number of Pixels
Amygdala + piriform cortex	165.2 ± 2.7
Dorsal hippocampus	135.0 ± 2.4
Parietal cortex	112.1 ± 1.7

Regions of interest drawn on the images using a free hand in both temporal lobes consisted of the amygdaloid nucleus and piriform cortex, and also the parietal cortices on coronal scans, and the dorsal hippocampi bilaterally on axial scans, in each animal (Fig 1B). Mean signal intensities were measured in regions of interest on DW and T2W images. Signal intensity data were presented as a function of time and as two ratios. First, treated/control ratio is tabulated as mean signal intensity in KA-treated rats divided by the average intensity of corresponding regions of interest in control rats. Second, the signal intensity ratio of the amygdala and piriform cortex to the parietal cortex is demonstrated to highlight the difference in signal intensity between a limbic structure and a nonlimbic cortex.

The apparent diffusion coefficient (ADC) was determined for region of interest from mean intensity by the equation:

$$ADC = \ln(So/Sn)/b$$

where Sn is the mean intensity for a DW image, and So is the equilibrium intensity for a corresponding T2W image (18, 19). An increased signal intensity on a DW image correlates with a reduction of ADC.

The Mann-Whitney *U* test was performed between the data of the rats with seizures and those of control

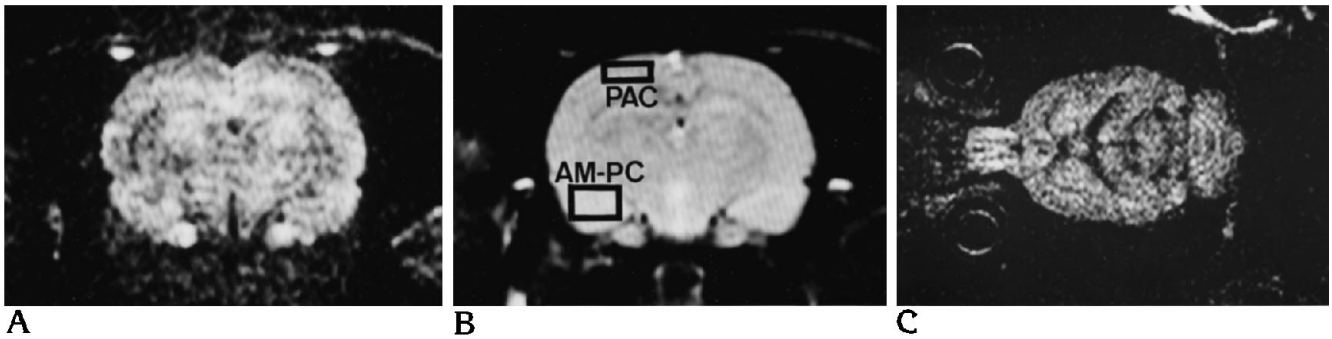

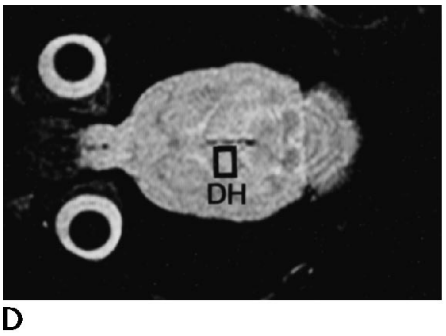

Fig 1. Typical control DW and T2W images in coronal (*A* and *B*) and horizontal (*C* and *D*) sections. Regions of interest are indicated by *boxes* on the T2W images in *B* and *D*. *AM-PC* indicates amygdala and piriform cortex area; *PAC*, parietal cortex; and *DH*, dorsal hippocampus.

animals. All values are mean ± SE. A *P* value less than .05 was considered significant.

At various times after completing MR imaging, the animals were deeply anesthetized with 60 mg/kg intraperitoneal pentobarbital and perfused through the left cardiac ventricle with saline. Perfusion was continued with 100 mL of 0.1 M phosphate-buffered 4% formaldehyde (pH 7.4). Three animals were killed at 5 hours, one at about 26 hours, one at 3 days, and two at 7 days after KA injection. The brains were stored in the fixative at 4°C for several days and embedded in paraffin. Sections of 5 μm were stained with hematoxylin and eosin.

Results

An intraperitoneal injection of KA induced limbic and generalized seizures within 2 hours in all the animals treated. The measurements of arterial blood gas did not show hypoxic reaction in the three KA-treated animals either immediately after induction of anesthesia after sustained seizures or at the end of the MR studies (Table 1). The treated animals had mild acidosis after 1-hour sustained seizures and imaging studies.

MR Imaging

Typical DW and T2W images are presented in Figure 1. As early as 1 hour after the initiation of sustained seizures with KA, DW images demonstrated an increased signal in the amygdala and piriform cortex of all seven animals examined, whereas T2W images showed signal intensities essentially similar to the control brain (Fig 2A and B). At 24 hours after KA, DW images showed a further increase in contrast between the corresponding area and the parietal cortex because of the progressively increased signal of

TABLE 1: Arterial blood gas data, mean ± SE

	Baseline	Seizures/Anesthesia	After MR Study
Rats with induced seizures (KA) (n = 3)			
$<Po_2$, mm Hg	94.0 ± 6.6	140.4 ± 31.3	144.2 ± 8.4
Pco_2, mm Hg	38.5 ± 3.3	21.0 ± 4.6	28.8 ± 1.4
pH	7.412 ± 0.017	7.273 ± 0.093	7.337 ± 0.041
Control rats (saline) (n = 3)			
Po_2, mm Hg	89.7 ± 6.9	. . .	194.5 ± 14.1
Pco_2, mm Hg	33.8 ± 1.1	. . .	33.8 ± 2.9
pH	7.466 ± 0.03	. . .	7.468 ± 0.022

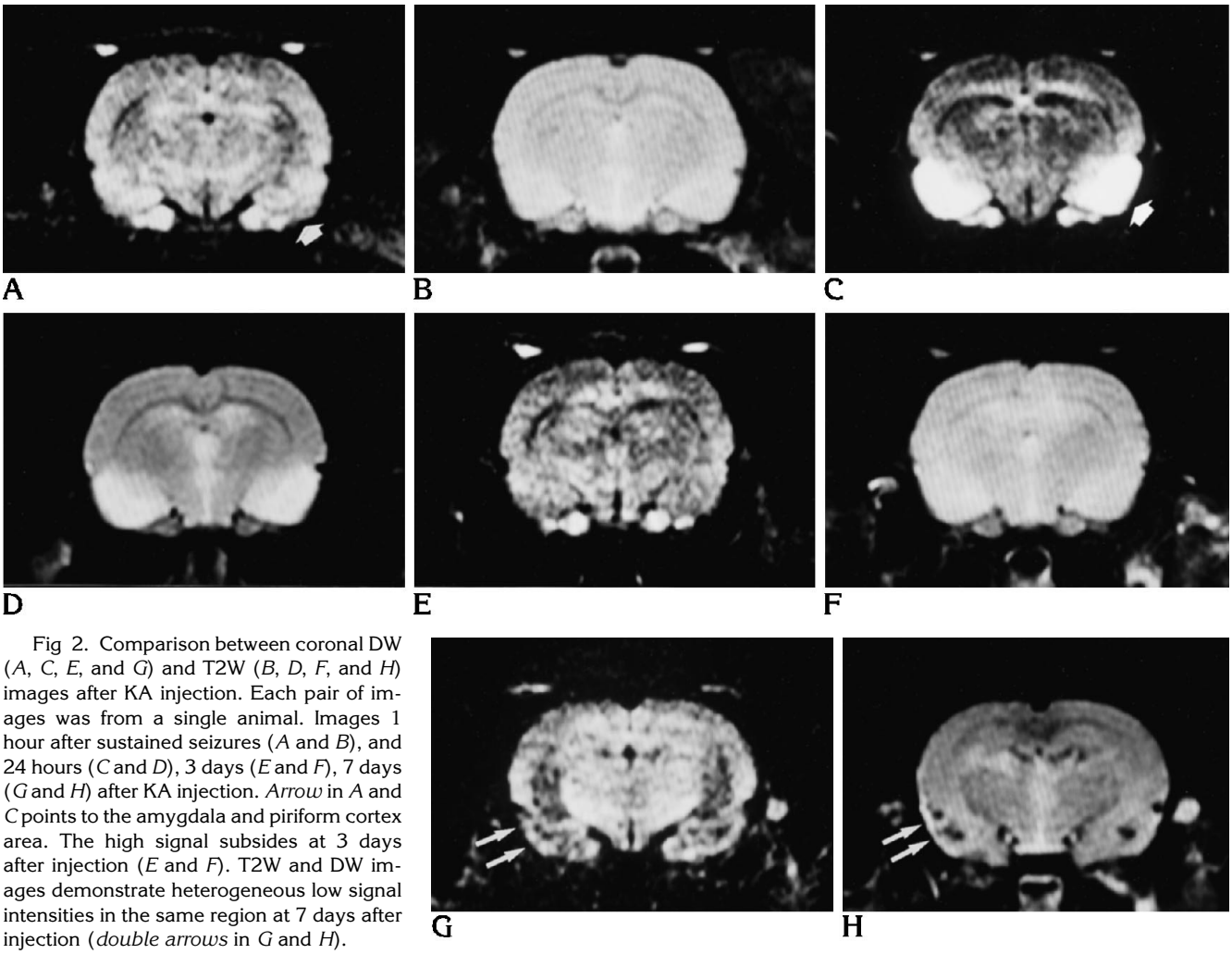

Fig 2. Comparison between coronal DW (*A*, *C*, *E*, and *G*) and T2W (*B*, *D*, *F*, and *H*) images after KA injection. Each pair of images was from a single animal. Images 1 hour after sustained seizures (*A* and *B*), and 24 hours (*C* and *D*), 3 days (*E* and *F*), 7 days (*G* and *H*) after KA injection. *Arrow* in *A* and *C* points to the amygdala and piriform cortex area. The high signal subsides at 3 days after injection (*E* and *F*). T2W and DW images demonstrate heterogeneous low signal intensities in the same region at 7 days after injection (*double arrows* in *G* and *H*).

the former in all four rats studied (Fig 2C). At the same time, T2W images also demonstrated an increase in signal intensity in the same area, although less remarkably than the DW images (Fig 2D). The changes in signals on both DW and T2W images subsided 3 (three rats) to 7 (two rats) days after the injection of KA (Fig 2E–H). Seven days after the initial sustained seizures, the amygdala and piriform cortex showed heterogeneous and slightly low-intensity signals on DW and T2W images (Fig 2G and H). On the other hand, axial sections did not show changes either on DW or on T2W images taken immediately, 24 hours, 3 days, and 7 days after sustained seizures (figure not shown).

Table 2 shows the change in treated/control ratio of signal intensities in DW and T2W images. The treated DW signal intensity increased to as much as twice that of control in the amygdala and piriform cortex. The dorsal hippocampus on the axial scan showed a tendency of paradoxical decrease in the treated/control ratio of diffusion signal intensity 1 hour after the initiation of sustained seizures, and slight increase in the treated/control ratio at 24 hours after injection. These changes in the dorsal hippocampus, however, did not reach statistical significance. On the other hand, T2 signal intensity of treated rats increased maximally to 34% higher than the control value in the amygdala and piriform cortex area at 24 hours. The ratios of signal intensity in the amygdala and piriform cortex to that in the parietal cortex show a significant change in DW images one hour and 24 hours after the seizures (Figs 3 and 4). The signal ratios of T2W images show a mild increase in contrast between the two areas only at 24 hours after the seizures.

TABLE 2: MR signal intensity ratio of treated to control rats, mean ± SE

	1 h	24 h	3 d	7 d
Diffusion-weighted				
Amygdala + piriform cortex	116.1 ± 4.9†	209.2 ± 27†	112.2 ± 3.2*	104.6 ± 6.2
Dorsal hippocampus	88.8 ± 2.5	118.4 ± 6.7	106.3 ± 9.2	95.4 ± 2.9
Parietal cortex	102.3 ± 3.9	115.5 ± 5.2	111.3 ± 2.6	108.5 ± 4.2
T2W				
Amygdala + piriform cortex	95.6 ± 1.0	134.1 ± 7.0†	105.9 ± 1.3	98.6 ± 2.9
Dorsal hippocampus	94.9 ± 1.5	113.1 ± 3.8	108.0 ± 4.1	97.0 ± 2.4
Parietal cortex	94.5 ± 1.9	110.9 ± 3.7	103.9 ± 2.2	97.1 ± 2.0

* $P < .05$.
†$P < .01$ (Mann-Whitney *U* test).

ADC

The changes in mean values of the ADC of the parietal cortex, the amygdala and piriform cortex, and the dorsal hippocampus are shown as a function of time after KA injection in Figure 5. After 1-hour sustained seizures, the mean ADC values of the amygdala and piriform cortex were 15% lower than those of control rats ($P < .01$). The ADC of these areas further fell an additional 15% at 24 hours ($P < .01$), and nearly returned to the control level on the third day. In contrast, the changes in ADC were not significant in the parietal cortex or the dorsal hippocampus.

Histologic Findings

Pyknotic neurons were found scattered in the amygdala and the piriform cortex at about 5 hours after KA injection. From 24 hours to 3 days after the injection, the neuropile became progressively disrupted, forming a vacuolated layer in the piriform cortex (Fig 6). The histologic changes showed clear boundaries between the limbic and nonlimbic systems. Neurons of all amygdala nuclei were affected, but less severely than the piriform cortex. The piriform cortex showed progressive swelling and edema at 24 hours' survival time and eventually became necrotic, with occasional hemorrhagic disruption.

Discussion

The present study demonstrates that DW MR images show focal changes in the rat brain after sustained seizures. An increase in signal first appeared and progressed in amygdala and piriform cortex on the DW images immediately af-

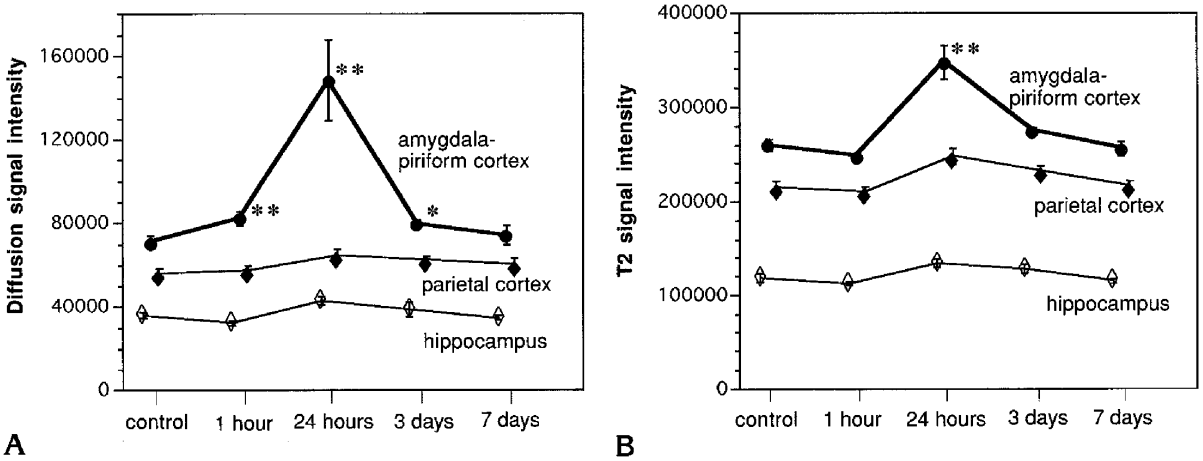

Fig 3. Mean signal intensity values of regions of interest in a DW image (*A*) and in a T2W image (*B*) plotted as a function of time. DW images demonstrate significant changes in signal intensity value of the amygdala and piriform cortex region at 1 hour, 24 hours, and 3 days in DW images; T2W images show a significant increase in signal intensity value of the same region only at 24 hours. (Values are mean ± SE. Number of specimens are 8 for control, 7 for 1 hour after status, 4 for 24 hours, 3 for 3 days, and 2 for 7 days after injection. A pair of regions of interest was evaluated in the bilateral hemispheres of each rat. *Asterisk* indicates $P < .05$; *double asterisk*, $P < .01$, Mann-Whitney *U* test.)

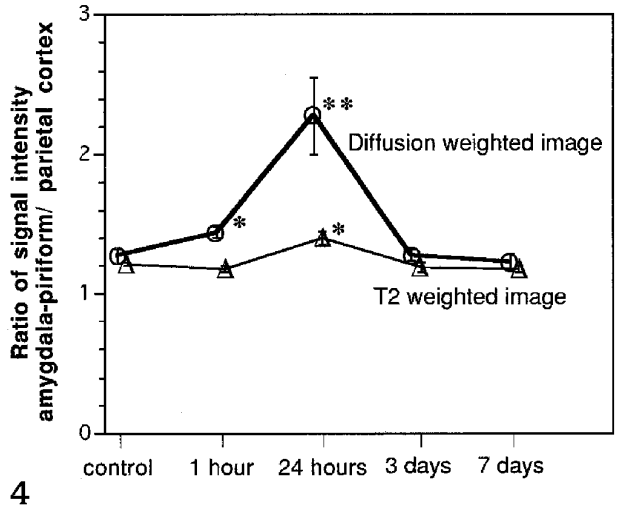

4

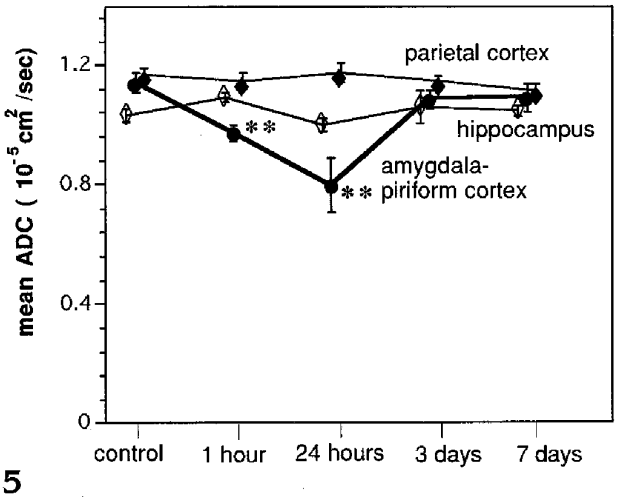

5

Fig 4. Signal intensity ratios between regions of interest in the amygdala and piriform cortex region and in the parietal cortex are plotted as a function of time. The DW image line shows significant increases in the ratio at 1 hour and 24 hours, whereas the T2W image line indicates a significant but less prominent increase at 24 hours. (Values are mean ± SE. Number of specimens are the same as Figure 3. *Asterisk* indicates $P < .05$; *double asterisk,* $P < .01$.)

Fig 5. Mean ADCs as a function of time after the initiation of sustained seizures by KA injection. In the amygdala and piriform cortex area, decreases in mean ADCs are significant at 1 and 24 hours after the sustained seizures when compared with control value. (Values are mean ± SE. Number of specimens are the same as Figure 3. *Asterisk* indicates $P < .05$; *double asterisk*, $P < .01$.)

ter 1-hour sustained seizures. The conventional T2W images demonstrated increased signal intensities in the corresponding area from 24 hours after KA injection. These changes were not induced by systemic hypoxia, because the animals did not have hypoxic conditions 1 hour after the seizures and after the subsequent MR studies. They showed acidosis, which was caused by severe systemic muscle contraction during the 1-hour prolonged convulsive seizures, and we did not correct it during the studies.

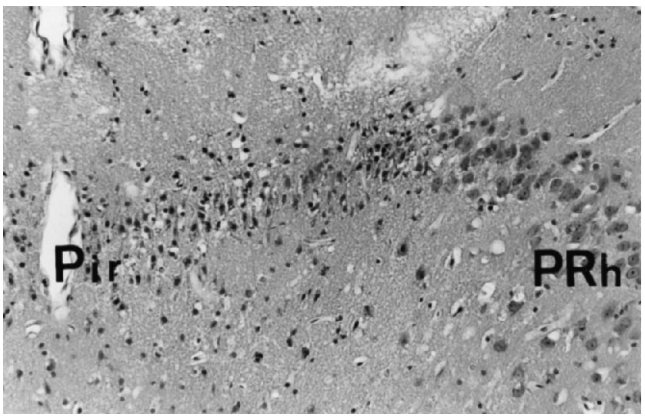

Fig 6. Photomicrograph showing the piriform cortex (*Pir*) at 24 hours after KA injection and sustained seizures. Note numerous pyknotic neurons with prominent vacuolation in the neuropile. The abnormality is less severe in neurons of the perirhinal cortex (*PRh*) (hematoxylin-eosin stain, magnification ×100).

One of the important aims for imaging in experimental epilepsy is to produce tissue changes that can be used to validate the correlation between the results of advanced radiologic imaging and histopathologic analysis. To provoke sustained seizures, we used KA, a well-known excitotoxic analog of glutamate that induces sequential and focal histologic changes throughout the limbic system by systemic treatment or microinjection into the brain (15, 16, 20, 21). Our histologic findings in the early phase were consistent with the description in literature; even at 5 hours' survival time, pyknotic neuronal changes and neuropile vacuolation were encountered in the amygdaloid complex, piriform cortex, and CA3 and CA4 of the hippocampus. Dilated dendrites and glial filaments have been observed with electron microscopy in the affected areas as an acute neuropathologic reaction to systemic treatment with KA (21). At 24 hours and 3 days, our histologic study showed that the piriform cortex seemed progressively swollen and vacuolated, then eventually became totally disrupted and formed extracellular edema, parenchymal necrotic change, and patchy hemorrhage. These findings are in agreement with previous reports (15, 20, 21). The pattern of abnormalities on our serial DW images seems to be concordant with the histopathologic sequence of the dam-

age in the amygdala and piriform cortex after seizures induced by KA: mild high signal intensity with the histologic focal vacuolation of the neuropile just after the sustained seizures; high-contrast area with progressing vacuolation at 24 hours, turning into mild hypointensity with a shift to extracellular edema at 3 days, and heterogeneous hypointensity with focal necrosis and hemorrhage in the region at 7 days.

As for the other compartments of the limbic system, we did not detect definitive changes as in the amygdala and piriform cortex either on DW or T2W images, although we tried to demonstrate the entorhinal cortex or the ventral or dorsal hippocampus using thin axial scanning. This result may be a consequence of the difference in response between the piriform cortex and other limbic structures after sustained seizures by KA, histologic findings showing more destructive changes in the former (20, 21). The winding anatomic alignment of nerve cell layers in rich and multidirectional fibers may be another explanation for the ambiguity of the changes in the hippocampus on DW MR images. It may also be caused by the limited volume of the injured hippocampal neuronal tissue (20), relative to the resolution of our equipment.

The direct neurotoxicity of glutamate analogs in the brain was previously studied with DW imaging. A study in a rat pup model using *N*-methyl-D-aspartate microinjection revealed that the primary lesion was hyperintense on DW images as early as 15 minutes after injection, whereas the lesion was not observed on T2W images until 24 hours after the injection (8). It was also shown in a model of microinjection of KA into the rat striatum that the secondary hyperintense area in the ipsilateral amygdala and piriform cortex was highlighted on DW MR images 24 hours after the lesioning (7). These models, which use stereotactic injection into an anatomic focus, are appropriate for exploring the direct effects or toxicity of glutamate analogs in the central nervous tissue. The systemic injection of an excitatory amino acid as applied in this study provides a less invasive and more physiologic model for studying neuronal injuries propagated in the epileptic brain.

The ADC values of the cortex in control animals were in agreement with the values in the literature (22–24). Significant falls in the ADC were observed in the amygdala and piriform cortex in our model 1 and 24 hours after the sustained seizures. DW MR imaging is performed by applying bipolar pulsed gradients in such a way as to sensitize the image to small magnitudes of proton motion. Controversies still exist concerning the biological basis of changes in the signal intensity and ADC in pathologic conditions. In animal models of focal brain ischemia, the ADC in the affected region starts to decrease within 10 to 30 minutes after the occlusion of the middle cerebral artery (13, 23, 24), being highly correlated with the postmortem area of infarction (13, 22). The early ADC reduction in the ischemic brain is presumed to represent the rapid shift of water between extracellular and intracellular compartments (22, 24–26). Other potential mechanisms for the early ADC changes in ischemia include a local reduction of tissue temperature, reduced perfusion, or a change in membrane permeability (10, 27, 28). Benveniste and colleagues supported the cytotoxic edema theory with their study of the rat brain tissue exposed to ischemia, ouabain, glutamate, or *N*-methyl-D-aspartate (22). Recently, Latour et al explained that the dominant contribution to the drop in diffusion coefficient came from a reduction of the extracellular volume fraction rather than a change in the membrane permeability, using effective medium theory in packed erythrocytes (28).

The proton movements in a region injured by sustained seizures have different characteristics from those in focal ischemia; there is no cessation of perfusion, severe energy depletion, or fall in the tissue temperature that might result in an ADC decrease in ischemic lesions. Systemic administration of KA is known to cause increases in local cerebral blood flow in the hippocampus, the amygdala, and the cortex of the rat brain (29), and KA-induced seizure models have shown marked increases of local cerebral glucose use in the limbic system (the hippocampus, the amygdaloid complex, the endopiriform nuclei, and the piriform cortex) (16, 20, 29). The significant decrease we observed in the ADC in the amygdala and piriform cortex might reflect the regional shift of water into the intracellular space, which has been histologically proved in the seizure model with KA injection. Thereafter, an increase in capillary perfusion, tissue necrosis, and/or extracellular edema to a various extent through the limbic system may explain the returning increase in ADC later developed in this study.

A recent study showed that the ADC of the rat neocortex declined as much as 15% without distinguished changes in DW images after intraperitoneal injection of a γ-aminobutyric acid receptor blocker under generalized anesthesia (9). The severity and the regional distribution of the ADC change in this model were not compatible with our result. The discrepancies might be explained by the facts that the actual drastic seizures were elicited in our unanesthetized model, and that the convulsant drugs, a γ-aminobutyric acid receptor blocker and a glutamate agonist, act on nervous tissue by their specific mechanisms and bring forth different morphologic changes in their characteristic distributions in the brain (20).

DW MR is subject to many questions (27, 30, 31). However, it can provide acute indications of in vivo tissue diffusion coefficients, which might contribute to understanding dynamic aspects of the brain after seizures. A sustained seizure may be another challenging subject for study in the field of DW MR.

References

1. Stone JL, Hughes JR, Barr A, Tan W, Russell E, Crowell RM. Neuroradiological and electroencephalographic features in a case of temporal lobe status epilepticus. *Neurosurgery* 1986;18:212–216
2. Kramer RE, Lüders H, Lesser RP, et al. Transient focal abnormalities of neuroimaging studies during focal status epilepticus. *Epilepsia* 1987;28:528–532
3. Horowitz SW, Merchut M, Fine M, Azar-Kia B. Complex partial seizure-induced transient MR enhancement. *J Comput Assist Tomogr* 1992;16:814–816
4. Warach S, Levin JM, Schomer DL, Holman BL, Edelman RR. Hyperperfusion of ictal seizure focus demonstrated by MR perfusion imaging. *AJNR Am J Neuroradiol* 1994;15:965–968
5. Karlik SJ, Stavraky RT, Taylor AW, Fox AJ, McLachlan RS. Magnetic resonance imaging and 31P spectroscopy of an interictal cortical spike focus in the rat. *Epilepsia* 1991;32:446–453
6. Nakasu Y, Kimura R, Handa J, Uemura S, Morikawa S, Inubushi T. Magnetic resonance imaging in status epilepticus elicited by kainate in rats. *Jpn J Psychiatry Neurol* 1993;47:406–407
7. King MD, van Bruggen N, Ahier RG, et al. Diffusion-weighted imaging of kainic acid lesions in the rat brain. *Magn Reson Med* 1991;20:158–164
8. Verheul HB, Balazs R, Berkelbach van der Sprenkel JW, Tulleken CAF, Nicolay K, van Lookeren Campagne M. Temporal evolution of NMDA-induced excitoxicity in the neonatal rat brain measured with 1H nuclear magnetic resonance imaging. *Brain Res* 1993; 618:203–212
9. Zhong J, Petroff OAC, Prichard JW, Gore JC. Changes in water diffusion and relaxation properties of rat cerebrum during status epilepticus. *Magn Reson Med* 1993;30:241–246
10. Moseley ME, Cohen Y, Mintorovitch J, et al. Early detection of regional cerebral ischemia in cats: comparison of diffusion- and T2-weighted MRI and spectroscopy. *Magn Reson Med* 1990;14: 330–346
11. Minematsu K, Li L, Fisher M, Sotak CH, Davis MA, Fiandaca MS. Diffusion-weighted magnetic resonance imaging: rapid and quantitative detection of focal brain ischemia. *Neurology* 1992;42:235–240
12. Warach S, Chien D, Li W, Ronthal M, Edelman RR. Fast magnetic resonance diffusion weighted imaging of acute human stroke. *Neurology* 1992;42:1717–1723
13. Kucharczyk J, Vexler ZS, Roberts TP, et al. Echo-planar perfusion-sensitive MR imaging of acute cerebral ischemia. *Radiology* 1993;188:711–717
14. Mayer ML, Westbrook GL. Cellular mechanisms underlying excitotoxicity. *Trends Neurosci* 1987;10:59–61
15. Coyle JT. Neurotoxic action of kainic acid. *J Neurochem* 1983; 41:1–11
16. Tanaka T, Tanaka S, Fujita T, et al. Experimental complex partial seizures induced by a microinjection of kainic acid into limbic structures. *Progr Neurobiol* 1992;38:317–334
17. Moseley ME, Cohen Y, Kucharczyk J, et al. Diffusion-weighted MR imaging of anisotropic water diffusion in cat central nervous system. *Radiology* 1990;176:439–445
18. Le Bihan D, Breton E, Lallemand D, Grenier P, Cabanis E, Laval-Jeantet M. MR imaging of intravoxel incoherent motions: application to diffusion and perfusion in neurologic disorders. *Radiology* 1986;161:401–407
19. Johnson GA, Maki JH. In vivo measurement of proton diffusion in the presence of coherent motion. *Invest Radiol* 1991;26:540–545
20. Ben-Ari Y, Tremblay E, Riche D, Ghilini G, Naquet R. Electrographic, clinical and pathological alterations following systemic administration of kainic acid, bicuculline or pentetrazole: metabolic mapping using the deoxyglucose method with special reference to the pathology of epilepsy. *Neuroscience* 1981;6:1361–1391
21. Schwob JE, Fuller T, Price JL, Olney JW. Widespread patterns of neuronal damage following systemic or intracerebral injections of kainic acid: a histological study. *Neuroscience* 1980;5:991–1014
22. Benveniste H, Hedlund LW, Johnson GA. Mechanism of detection of acute cerebral ischemia in rats by diffusion-weighted magnetic resonance microscopy. *Stroke* 1992;23:746–754
23. Pierpaoli C, Righini A, Linfante I, Tao-Cheng JH, Alger JR, Di Chiro G. Histopathologic correlates of abnormal water diffusion in cerebral ischemia: diffusion-weighted MR imaging and light and electron microscopic study. *Radiology* 1993;189:439–448
24. Bizzi A, Righini A, Turner R, et al. MR of diffusion slowing in global cerebral ischemia. *AJNR Am J Neuroradiol* 1993;14:1347–1354
25. Le Bihan D, Breton E, Lallemand D, Aubin M-L, Vignaud J, Laval-Jeantet M. Separation of diffusion and perfusion in intravoxel incoherent motion MR imaging. *Radiology* 1988;168:497–505
26. Knight RA, Ordidge RJ, Helpern JA, Chopp M, Rodolosi LC, Peck D. Temporal evolution of ischemic damage in rat brain measured by proton nuclear magnetic resonance imaging. *Stroke* 1991;22: 802–808
27. Fisher M, Sotak CH. Diffusion-weighted MR imaging and ischemic stroke: commentary. *AJNR Am J Neuroradiol* 1992;13:1103–1105
28. Latour LL, Svoboda K, Mitra PP, Sotak CH. Time-dependent diffusion of water in a biological model system. *Proc Natl Acad Sci USA* 1994;91:1229–1233
29. Celik G, Graham DI, Kelly PAT, McCulloch J. On the mechanism of kainic acid neurotoxicity. *J Cereb Blood Flow Metab* 1981; 1(Suppl 1):S102–103
30. Pickens DR. Perfusion/diffusion quantitation with magnetic resonance imaging. *Invest Radiol* 1992;27(Suppl 2):S12–17
31. Helpern JA. Editorial comment. *Stroke* 1994;25:848